SPIN PHYSICS WITH POLARIZED ^{3}HE

WOLFGANG KORSCH

Department of Physics & Astronomy,
University of Kentucky, Lexington,KY 40506, USA
E-mail: korsch@pa.uky.edu

Polarized helium-3 ($^3\vec{\mathrm{He}}$) gas targets have evolved to a standard tool on extracting fundamental properties of the neutron. The present status of its applicability on the extraction of high precision neutron spin structure information will be described.

1. Introduction

In the late 1980's the EMC collaboration measured the proton spin structure function $g_1^p(x, Q^2)$ using inclusive deep inelastic polarized muon - proton scattering at CERN [1]. Assuming the validity of the Bjorken (Bj) sum rule [2] a spin flavor decomposition was performed. The surprising result was that only about 10% of the proton's spin was carried by the *up* and *down* quarks. The EMC result implied that the Ellis-Jaffe sum rule [3] was violated and the *strange* quarks seemed to be polarized in opposite direction to the polarization vector of the protons ($\approx$ -7%). This, at that time very surprising result, triggered enormous experimental and theoretical efforts to study the spin structure of the nucleon in great detail. Since the original results were obtained on the proton they had to be complemented by similar measurements on the neutron. However, the extraction of neutron properties is less straightforward, since they can only be accessed by means of light nuclei. As a consequence the development of dense and highly polarized *deuteron* and *helium-3* targets became crucial. Deuterons have the advantage of being simplest system of two bound nucleons, but they are nuclear spin-1 systems, implying that any asymmetry measurement has to be corrected for contributions from the proton. The other commonly used polarized target, $^3\vec{\mathrm{He}}$, has the advantage that corrections of measured asymmetries due to contributions from the proton are small, but nuclear effects, such as Fermi motion or off-shellness, have to be taken into account.

Table 1 summarizes the progress in $^3\vec{\mathrm{He}}$ target technology. Note that this table comprises the status of external and internal $^3\vec{\mathrm{He}}$ targets. It is evident that there has been a steady continuous improvement in target polarization and, in the case of external targets, in density. The limits have not been reached yet. However, the numbers show that $^3\vec{\mathrm{He}}$ targets are very suitable for high precision studies on ^{3}He structure and fundamental properties of the neutron, such as electric charge and magnetic current distributions as well as spin structure studies.

Lab/Exp	year	beam	$I[\mu A]$	$\rho[cm^{-2}]$	$\mathcal{L}[s^{-1}cm^{-2}]$	P_t	Physics
MIT/Bates (I)	90	e^-	6	$7.5 \cdot 10^{20}$	$2.8 \cdot 10^{34}$	0.19	G_E^n, ^{3}He
MIT/Bates (IIa)	90	e^-	11	$1.1 \cdot 10^{19}$	$7.6 \cdot 10^{32}$	0.30	G_E^n, ^{3}He
TRIUMF	91	p	$3.5 \cdot 10^{-3}$	$2.0 \cdot 10^{21}$	$4.4 \cdot 10^{31}$	0.60	^{3}He
SLAC (E142)	92	e^-	1.5	$7 \cdot 10^{21}$	$6.6 \cdot 10^{34}$	0.35	$g_{1,2}^n$, Γ_1^n
MIT/Bates (IIb)	93	e^-	25	$3.3 \cdot 10^{18}$	$5.1 \cdot 10^{32}$	0.38	G_M^n, ^{3}He
IUCF	93	p	70	$1.5 \cdot 10^{14}$	$6.6 \cdot 10^{28}$	0.46	^{3}He
HERMES	95	e^+	$20 \cdot 10^3$	$3.3 \cdot 10^{14}$	$4.1 \cdot 10^{31}$	0.46	g_1^n, Γ_1^n, GDH
NIKHEF	96	e^-	$80 \cdot 10^3$	$7 \cdot 10^{14}$	$3.5 \cdot 10^{32}$	0.50	G_E^n, ^{3}He
SLAC (E154)	95	e^-	1.5	$8 \cdot 10^{21}$	$7.5 \cdot 10^{34}$	0.38	$g_{1,2}^n$, Γ_1^n
MAMI	97	e^-	7	$5 \cdot 10^{20}$	$2.2 \cdot 10^{32}$	0.50	G_E^n, ^{3}He
JLab	98-??	e^-	(10-15)	$\geq 8 \cdot 10^{21}$	$6.7 \cdot 10^{35}$	≥ 0.35	$g_{1,2}^n$, A_1^n GDH, $G_{E,M}^n$
BLAST	03(?)	e^-	$(80 \cdot 10^3)$	$(7 \cdot 10^{14})$	$(3.5 \cdot 10^{32})$	(0.5)	$G_{E,M}^n$, ^{3}He

2. How to Extract Neutron Properties from $^3\vec{\mathrm{He}}$

Experimentally properties of the neutron can be extracted by performing inclusive or semi-inclusive scattering asymmetries in polarized lepton-^{3}He scattering and then correcting the results for the fact that the neutron is embedded in the ^{3}He nucleus. For example, aligning the target spins parallel or perpendicular to the momentum of the incoming leptons allows us to measure the following scattering asymmetries in deep inelastic scattering (DIS), if the leptons are longitudinally polarized and their helicity can be flipped:

$$A_{\parallel}^{^3He} = D' \cdot \left\{ (E + E' cos(\vartheta)) g_1^{^3He}(x, Q^2) - \frac{Q^2}{\nu} g_2^{^3He}(x, Q^2) \right\}$$
$$A_{\perp}^{^3He} = D' \cdot E' sin(\vartheta) \left\{ g_1^{^3He}(x, Q^2) + \frac{2E}{\nu} g_2^{^3He}(x, Q^2) \right\} \quad (1)$$

The factor D' contains the unpolarized structure functions $F_1(x, Q^2)$ and $F_2(x, Q^2)$ (or $R(x, Q^2)$) besides some kinematic quantities. If these unpolarized structure functions are known, the spin structure functions, $g_{1,2}^{^3He}(x, Q^2)$, can be extracted. The superscript '^{3}He' indicates that the

spin structure functions are measured on ^{3}He. Scopetta *et al.*[6] showed that the neutron spin structure functions $g^n_{1,2}(x, Q^2)$ can be extracted reliably by using the formula:

$$g^{^3He}_{1,2}(x, Q^2) = P_n g^n_{1,2}(x, Q^2) + 2P_p g^p_{1,2}(x, Q^2) \ , \tag{2}$$

where P_n (0.86 ± 0.02) is the polarization of the neutron inside ^{3}He and P_p (0.02 ± 0.01) is the corresponding proton polarization. These polarization essentially take care of the S'- and D-states in the helium-3 wave function. Recently Bissey *et al.* included the effects of the Δ isobar, pions, vector mesons, off-shellness, as well as nuclear (anti)shadowing for $0.05 \lesssim x \lesssim 0.2$ [7]. See the contributions of M. Strikman to these proceedings and Ref. 7 for details. Fig. 1 shows a compilation of the spin structure function g^n_1 where the data were evolved to a common Q^2 of 4 GeV/c^2 assuming that the ratio g^n_1/F^n_1 is Q^2 independent. Eq. 2 was employed to extract g^n_1 whenever the target nucleus was $^3\vec{\mathrm{He}}$. No real difference between the extraction of g^n_1 from d/p (gray markers) or ^{3}He (black markers) can be noticed within the accuracy of the data. However, a slight enhancement of the g^n_1 data extracted from ^{3}He cannot be excluded. This could be an indication of remaining nuclear effects. More precise data is needed to confirm this observation. An independent test of theory and experiment is the

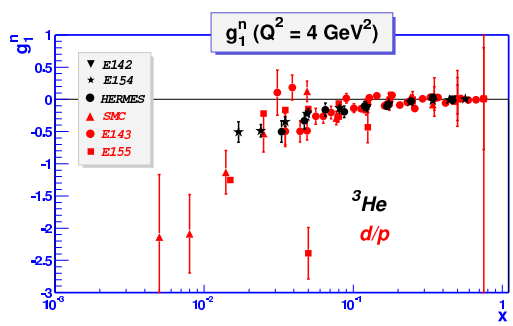

Figure 1. World data of g^n_1 evolved to $Q^2 = 4$ GeV/c^2.

determination of the *Bj* sum rule. At present the best value for this sum rule is:

$$\Gamma^p_1 - \Gamma^n_1(Q^2 = 5 \text{ GeV}^2) = 0.176 \pm 0.003 \pm 0.007(exp) \ \ (0.181 \pm 0.005(theo)) \tag{3}$$

when NLO QCD corrections up to α^3_s are taken into account. The difference between the theoretically expected value and the measured value is less than 5%. All existing data, i.e. including ^{3}He, were used which shows that corrections due to nuclear effects appear to be small.

3. χPT meets pQCD: The Gerasimov-Drell-Hearn (GDH) Sum Rule

It is generally accepted that QCD is the fundamental theory of strong interactions. Perturbative QCD (pQCD) has been extremely successful in describing DIS data where partonic degrees of freedom serve as a basis. At lower energies ($W \lesssim 2$ GeV) and $Q^2 \lesssim 1$ GeV^2/c^2 the partonic picture has to be replaced by a hadronic picture since now the participants of the interactions are baryons and mesons. Here lattice QCD becomes applicable. At very low momentum transfers, close to the real photon point, effective field theories, such as chiral perturbation theory χPT, can be used. χPT and pQCD can be derived from first principles and are therefore model independent. One of the few quantities where χ PT and pQCD can be employed to the same physics quantity is the *generalized* Gerasimov-Drell-Hearn (GDH) sum rule [4,5]. For real photon compton scattering this sum rule states that the spin-dependent cross-sections is related to the anomalous magnetic moment moment of the nucleon via:

$$I(Q^2=0) = \int_{\nu_{thresh}}^{\infty} \frac{d\nu}{\nu}(\sigma_{\uparrow\downarrow}(\nu) - \sigma_{\uparrow\uparrow}(\nu)) = -\frac{2\pi^2\alpha}{M_N}\kappa_N^2 \tag{4}$$

Eq. 4 was derived on very general grounds such as causality, an *unsubtracted* dispersion relation, and unitarity, together with a low energy theorem. An extension of the integral to non-zero values of Q^2 can be performed by taking the transverse part of the spin-dependent virtual photon cross-sections. Now we have a Q^2 dependent integral which can be evaluated theoretically using χPT techniques at low Q^2 and the operator product expansion (OPE) at large Q^2. Only a small region between about 0.2 GeV^2/c^2 $\lesssim Q^2 \lesssim$ 0.5 GeV^2/c^2 cannot be covered using these techniques. Often the difference in the spin dependent cross section is called σ'_{TT} and is related to the spin structure functions via:

$$\sigma'_{TT} = \frac{1}{2}(\sigma_{\uparrow\downarrow} - \sigma_{\uparrow\uparrow}) = \frac{4\pi^2\alpha}{M_N K}\big(g_1(x,Q^2) - \frac{Q^2}{\nu^2}g_2(x,Q^2)\big). \tag{5}$$

We measured the integral for six different values of Q^2 in a range from 0.1 GeV^2/c^2 to 0.9 GeV^2/c^2 using a polarized ^3He target in Hall A at Jefferson Lab. The $^3\vec{\mathrm{He}}$ target was operated at 10-12 atm and an average in-beam polarization of 35$\pm$0.014 was achieved. Both high resolution spectrometers (HRS) were used in single arm mode. The polarization of a longitudinally polarized electron beam ($P_b \approx 70\%$, $I = (10-15)\mu A$) was flipped at a rate of 1 Hz. The beam energy varied between 0.86 GeV and 5.06 GeV.

Data were taken from quasi-elastic kinematics through the resonance region up to an invariant mass W of about 2 GeV. We used Eq. 5 for the evaluation of the integrals, i.e. we determined the cross sections and spin structure functions directly from asymmetry measurements. This procedure was necessary since the unpolarized structure functions of the neutron are not well known in the resonance region. We applied the model of degli Atti and Scopetta *et al.* [6] to extract the neutron information from the ^{3}He data. Radiative corrections were performed using the program POLRAD [8]. Fig. 2 shows our results of the GDH integral for the neutron as a function of Q^2. This is the first measurement of the generalized GDH sum on the neutron in the resonance region. A striking Q^2 dependence can be observed in this region where the transition from the partonic to the hadronic picture takes place. The shaded region at very low Q^2 is the prediction of Bernard *et al.* [9]. The calulation was performed within the framework of "infrared regulated" χPT. The shaded region covers the estimated error in the theory due to uncertainties in low energy constants. The dashed curve is a HBχPT calculation by Ji and Osborne [10]. It is interesting to note that there has to be a minimum in the GDH integral somewhere between $Q^2 = 0.1$ GeV^2/c^2 and 0. This region will be the focus of a follow-up experiment which will run this fall in Hall A at Jefferson Lab [11].

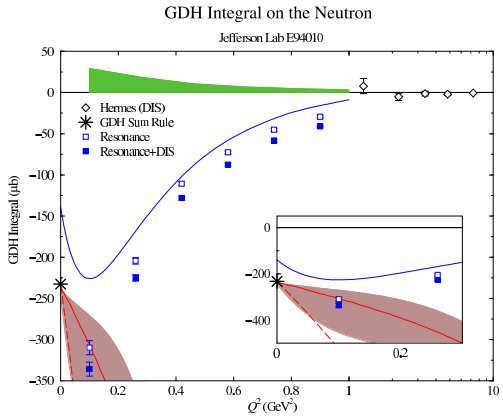

Figure 2. GDH integral for the neutron. Solid curve: "infrared regulated" χPT [9]. The shaded area is an estimate of the theoretical error. Dashed curve: standard HBχPT [10].

4. Neutron Spin Structure Functions

Due to the low beam energy at Jefferson Lab the maximum invariant mass W achievable is about 3.3 GeV. Therefore only a limited range in DIS region

can be probed. On the other hand, the achievable luminosities in combination with polarized targets are unprecedented. This allows for precision measurements at large values of the Bjorken variable x (up to $x \approx 0.6$) and low Q^2. Spin dependent measurements on the neutron at large x are of special interest since the present data for the virtual photon asymmetry, $A_1^n(x, Q^2)$, are consistent with zero at large x. This is in contradiction with expectations from pQCD and proton data where $A_1^p(x, Q^2)$ is large and positive as $x \to 1$. A high precision A_1^n experiment was performed using the Hall A $^3\vec{\mathrm{He}}$ target. See contribution to this workshop by X. Zheng.
In addition an experiment to study higher twist effects in the spin structure function $g_2^n(x, Q^2)$ at nearly constant x (≈ 0.2) was performed. Fig. 3 summarizes the present status of $g_2^n(x, Q^2)$. The need for more precise data is obvious. $g_2(x, Q^2)$ is a unique structure function since the leading twist

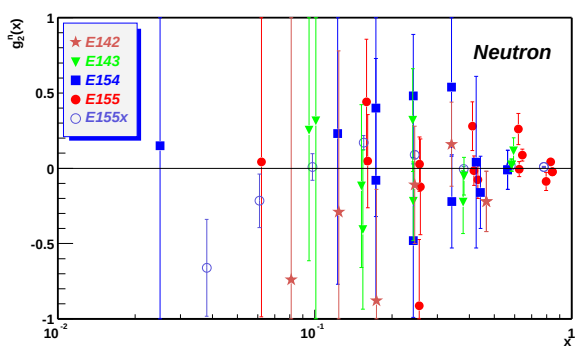

Figure 3. World data of $g_2^n(x, Q^2)$ (not evolved to a common Q^2).

contribution of the operator product expansion (OPE) can be separated according to the Wandzura-Wilczek relation [12]:

$$g_2^{WW}(x, Q^2) = -g_1(x, Q^2) + \int_{x'}^{1} \frac{dx'}{x'} g_1(x', Q^2) \ . \tag{6}$$

The leading twist term is completely determined by the twist-2 part of $g_1(x, Q^2)$, so that $g_2(x, Q^2) = g_2^{WW}(x, Q^2) + g_2^{HT}(x, Q^2)$, with $g_2^{HT}(x, Q^2)$ containing all the higher twist contributions. The higher twist components scale according to $\frac{1}{Q^{\{\tau\}}}$ (τ is the twist of the operator), i.e. their significance increases as Q^2 is reduced. Experiment E97-103 performed a high precision search for such higher twist effects in the following kinematic regime: $0.17 \leqslant x \leqslant 0.21$, 0.58 GeV^2/c^2 $\leqslant Q^2 \leqslant 1.36$ GeV^2/c^2, 3.82 GeV^2 $\leqslant W^2 \leqslant 6.03$ GeV^2. The statistical precision was improved by about a factor of 10

in this x range. For details on this experiment see the contribution by K. Kramer.

5. Summary

Thanks to the advent of the "proton spin crisis" in the late 1980's the development of $^3\vec{\mathrm{He}}$ targets experienced an enormous boost all over the world. Theoretical and experimental progress has been made and the neutron results extracted from $^3\vec{\mathrm{He}}$ are very complementary to the results extracted from deuterons, since the systematic errors are completely different. Accelerator laboratories like Bates, Jefferson, MAMI, and SLAC were able to extract precision data on $G^n_{E,M}$, $g^n_{1,2}$, and sum rules such as the GDH sum rule using $^3\vec{\mathrm{He}}$ targets. In the near future high precision measurements on the GDH at low Q^2, G^n_E at high Q^2, test of duality in g^n_1 at large x are planned at Jefferson Lab. The energy upgrade to 12 GeV will extent the present experimental program with $^3\vec{\mathrm{He}}$ significantly.

Acknowledgments

This work was supported by the US Department of Energy (DOE) under contracts DE-AC05-84ER40150 and DE-FG02-99ER41101, the US National Science Foundation (NSF), and the DOE/EPSCoR program.

References

1. J. Ashman *et al.*, EMC, Phys. Lett. B 206, 364 (1988).
2. J. D. Bjorken, Phys. Rev. 148, 1467 (1966); D 1, 1376 (1970).
3. J. Ellis and R. L. Jaffe, Phys. Rev. D 9, 1444 (1974); Phys. Rev. D 10, 1669(E) (1974).
4. S. B. Gerasimov, Sov. J. Nucl. Phys. 2, 430 (1966).
5. S. D. Drell and A. C. Hearn, Phys. Rev. Lett. 16, 908 (1966).
6. C. Ciofi degli Atti and S. Scopetta, Phys. Lett. B 44, 223 (1997).
7. F. Bissey *et al.*, Phys.Rev.C6 5, 064317 (2002).
8. T. V. Kuchto and N. M. Shumeiko, Nucl. Phys B 219, 412 (1983); I. V. Akushevich and N. M. Shumeiko, J. Phys. G 20, 513 (1994).
9. V. Bernard *et al.*, hep-ph/0203167.
10. X. D. Ji and J. Osborne, J. Phys. G 27, 127 (2001).
11. JLab proposal E97-110; J. P. Chen, A. Deur, and F. Garibaldi.
12. S. Wandzura and F. Wilczek, Phys. Lett. B 72, 195 (1977).